Supporting Information

Mahamid et al. 10.1073/pnas.0914218107

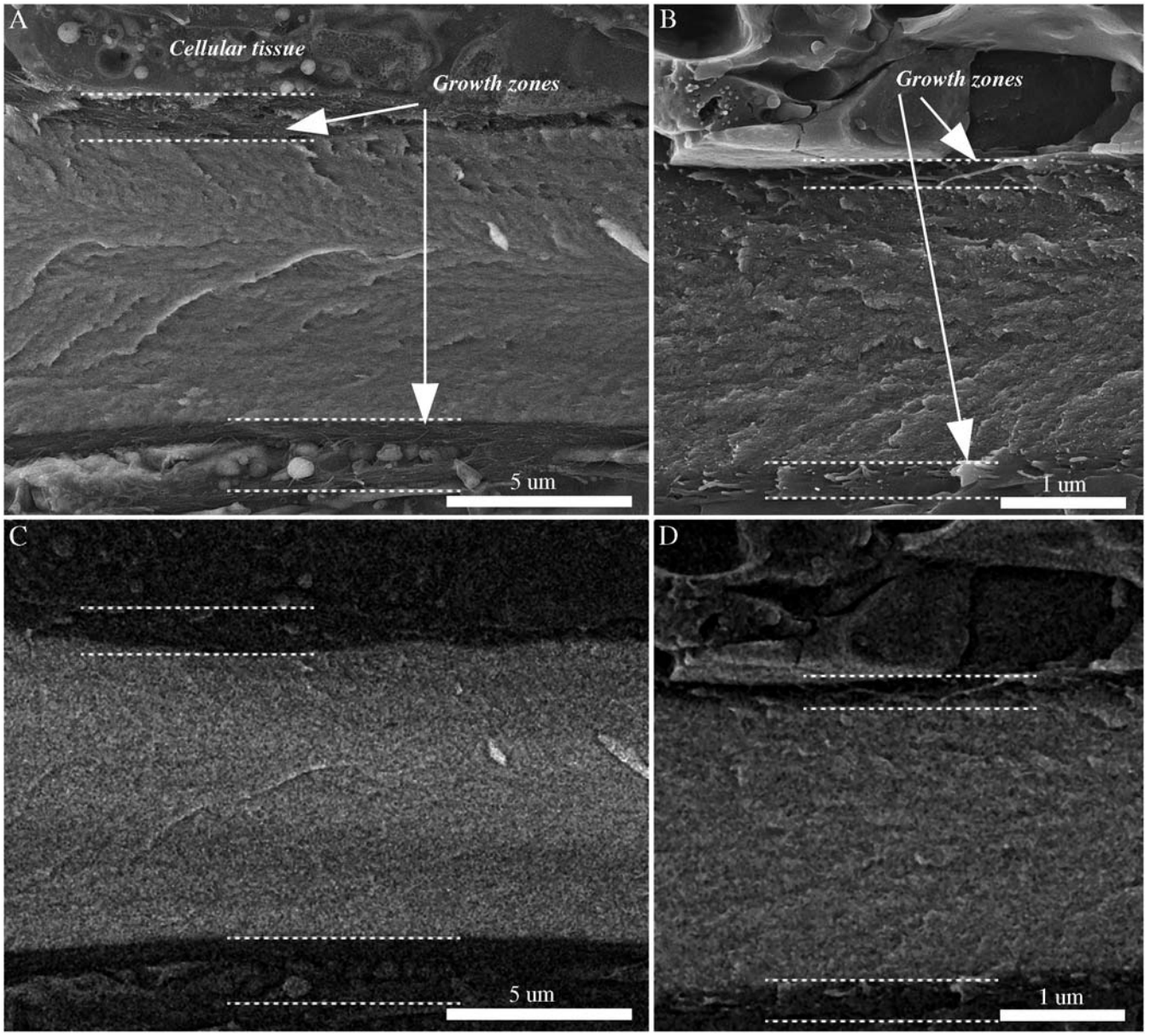

Fig. S1. Cryo-SEM micrographs of longitudinal fracture surfaces (blue plane in Fig. 1*B*, *x* direction) through native, high-pressure frozen mature bone (*A* and *C*) and younger (more distal) bone (*B* and *D*). The difference in bone thickness between the young and the mature bones reflects the continuous thickening of the segments (please note differences in scale bars between *A*,*C* and *B*,*D*). Growth zones at the bone circumference are indicated (*Arrows* and *Dashed Lines*). Backscattered electrons micrographs (*C* and *D*) show that the central part of the bone is mineralized both in the mature and distal bones, whereas the growth zones are yet to be mineralized.

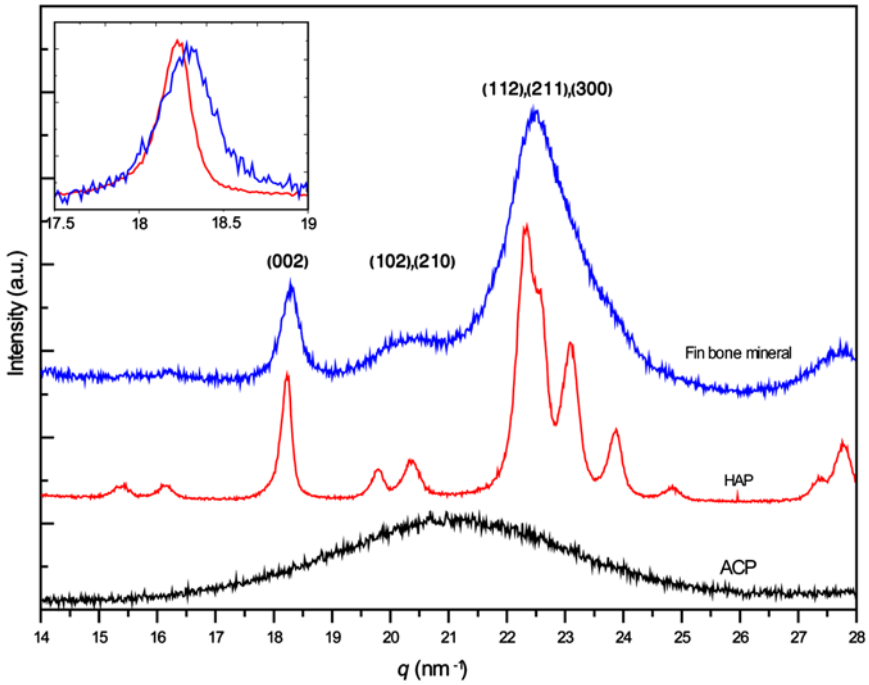

Fig. S2. Powder x-ray diffraction of synthetic hydroxyapatite (HAP: red), synthetic amorphous calcium phosphate (ACP: black), and bone mineral extracted from several TL zebrafish caudal fins (blue). The HAP powder produces typical diffraction peaks, whereas the peaks of bone carbonated hydroxyapatite are poorly resolved. (*Inset*) Comparison between the (002) reflection of synthetic and biogenic apatite. Bone apatite shows contraction of the *c* axis (*d* spacing = 3.43 Å) compared to the synthetic powder (*d* spacing = 3.44 Å), as shown by the peak shift of the blue curve to larger *q*. The contraction of the *c* axis is apparently an intrinsic property of the bone mineral. Such differences in unit cell dimensions have been previously reported for bone mineral and were attributed to the incorporation of ions such as magnesium and carbonate (1, 2). In addition, the bone apatite peak is substantially broadened because of the smaller size and lower crystallinity of the particles in bone. The (002) reflection of the bone samples measured within the tissue by using a synchrotron microbeam (μ-Spot beamline, BESSY II, HZB) show an even larger contraction of the *c* axis (*d* spacing = 3.41 ± 0.01 Å). The three indexed peaks produced by the bone mineral were used for peak fitting of the data measured in the microbeam experiments: 18.4 nm^{-1} (002), 20.5 nm^{-1} [unresolved (102) and (210)], and 22.5 nm^{-1} [unresolved (211), (112), and (300)]. Synthetic ACP produces a broad peak centered at 21.08 nm^{-1} (*d* spacing = 2.98 Å). For comparison, the *d* spacing of the amorphous phase in the fish bones measured in the microbeam experiments is approximately 3.23 Å. Hydroxyapatite powder was purchased from Biorad. ACP was precipitated by following Christoffersen et al. (3). Briefly, equal volumes of cold solutions of 0.02 M $CaCl_2$ and 0.012 Na_2HPO_4 were mixed for a minute and then filtered. The precipitate was washed with absolute ethanol and allowed to dry in a desiccator. The amorphous nature of the precipitate was confirmed by FTIR. Bone mineral was extracted as previously described (4): Freshly dissected caudal fins were washed with acetone to remove fatty tissue components and solute ions, followed by freezing with liquid nitrogen and crushing in an agate mortar. Sodium hypochlorite solution (6%) was added for 5 min at room temperature while manually stirring the suspension. The suspension was then transferred into Eppendorf tubes and centrifuged at 14 K rpm for 2 min to remove the supernatant. The pellet was washed three times with Milli-Q water saturated with calcium and phosphate and twice with 100% ethanol and allowed to dry. Powder x-ray diffraction was measured with a D8 diffractometer (Bruker AXS) in Bragg–Brentano geometry by using Cu K_α radiation (8.045 keV, $\lambda = 0.154$ nm).

1 Bigi A, et al. (1992) The role of magnesium on the structure of biological apatites. *Calcif Tissue Int* 50:439–444.
2 LeGeros RZ, Trautz OR, Klein E, LeGeros JP (1969) Two types of carbonate substitution in the apatite structure. *Experientia* 25:5–7.
3 Christoffersen J, Christoffersen MR, Kibalczyc W, Andersen FA (1989) A contribution to the understanding of the formation of calcium phosphates. *J Cryst Growth* 94:767–777.
4 Mahamid J, Sharir A, Addadi L, Weiner S (2008) Amorphous calcium phosphate is a major component of the forming fin bones of zebrafish: Indications for an amorphous precursor phase. *Proc Natl Acad Sci USA* 105:12748–12753.

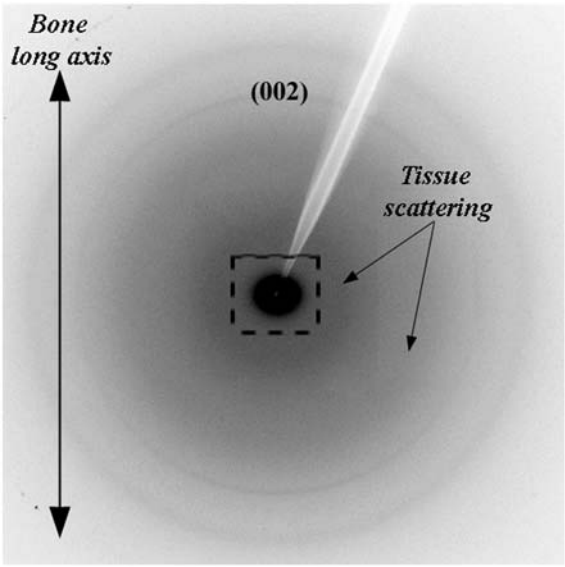

Fig. S3. Representative 2D scattering profile measured at the center of a distal bone segment, showing the main features dominating the bone scattering pattern: (002) crystalline reflection of carbonated apatite, diffuse scatter produced by the organic components of the tissue, and anisotropic small-angle scattering (delineated area) from the mineral. The mineral particles orientation in relation to the macroscopic bone long axis was not analyzed quantitatively, because we know that each segment is composed of areas with different fibril and mineral tilts on a scale that is smaller than the beam size (1). According to the preferred orientation of the (002) reflection parallel to the bone axis and to the anisotropy of the SAXS signal in the transverse direction, the mineral is on the average preferentially oriented parallel to the macroscopic long axis of the bone segments and fin rays.

1 Mahamid J, Sharir A, Addadi L, Weiner S (2008) Amorphous calcium phosphate is a major component of the forming fin bones of zebrafish: Indications for an amorphous precursor phase. *Proc Natl Acad Sci USA* 105:12748–12753.

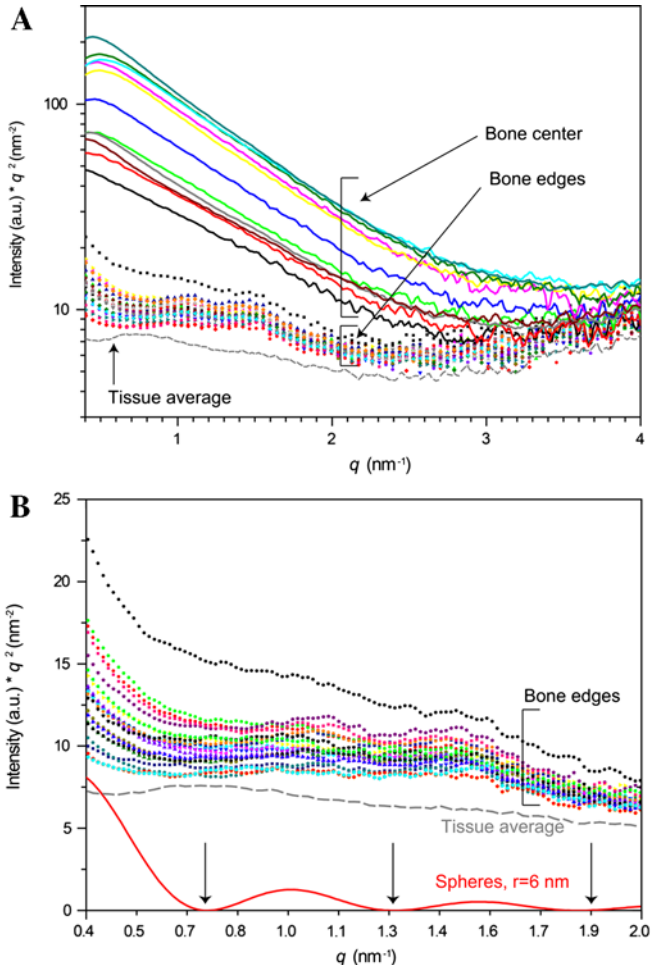

Fig. S4. Small-angle scattering profiles measured at the center of the bony ray (*Full Lines*), bone edges (*Dotted Lines*), and organic tissue (*Lowermost Dashed Gray Line*: average of 4 tissue measurements at different locations, artificially shifted in intensity for simplified visualization). To facilitate comparison, the curves were normalized by the mean intensity value for $q = 5$–17 nm^{-1} and the intensities were multiplied by q^2. (*A*) The *y* axis is logarithmic (to assist comparison between the different types of signals). Measurements taken at the center of the bone produce typical bone SAXS. The scattering from the bone edges shows characteristic oscillations that are not observed either in the tissue or in the mature bone. (*B*) Scattering profiles measured at the bone edges (*Dotted Lines*) and organic tissue (*Dashed Gray Line*) compared with the scattering function of monodispersed spheres with a radius of 6 nm (*Red Full Line*) (1). The *y* axis is linear. Arrows indicate the minima of the scattering function for spheres. The model shows a very good qualitative agreement with the growth zone mineral (the positions of the first two minima). Deviations might arise from other scattering contributions (organic tissue, mature mineral). For example, the black dotted curve (uppermost) likely contains a significant contribution from mature bone mineral particles.

1 Guinier A, Fournet G (1955) *Small-Angle Scattering of X-Rays* (Wiley, New York).

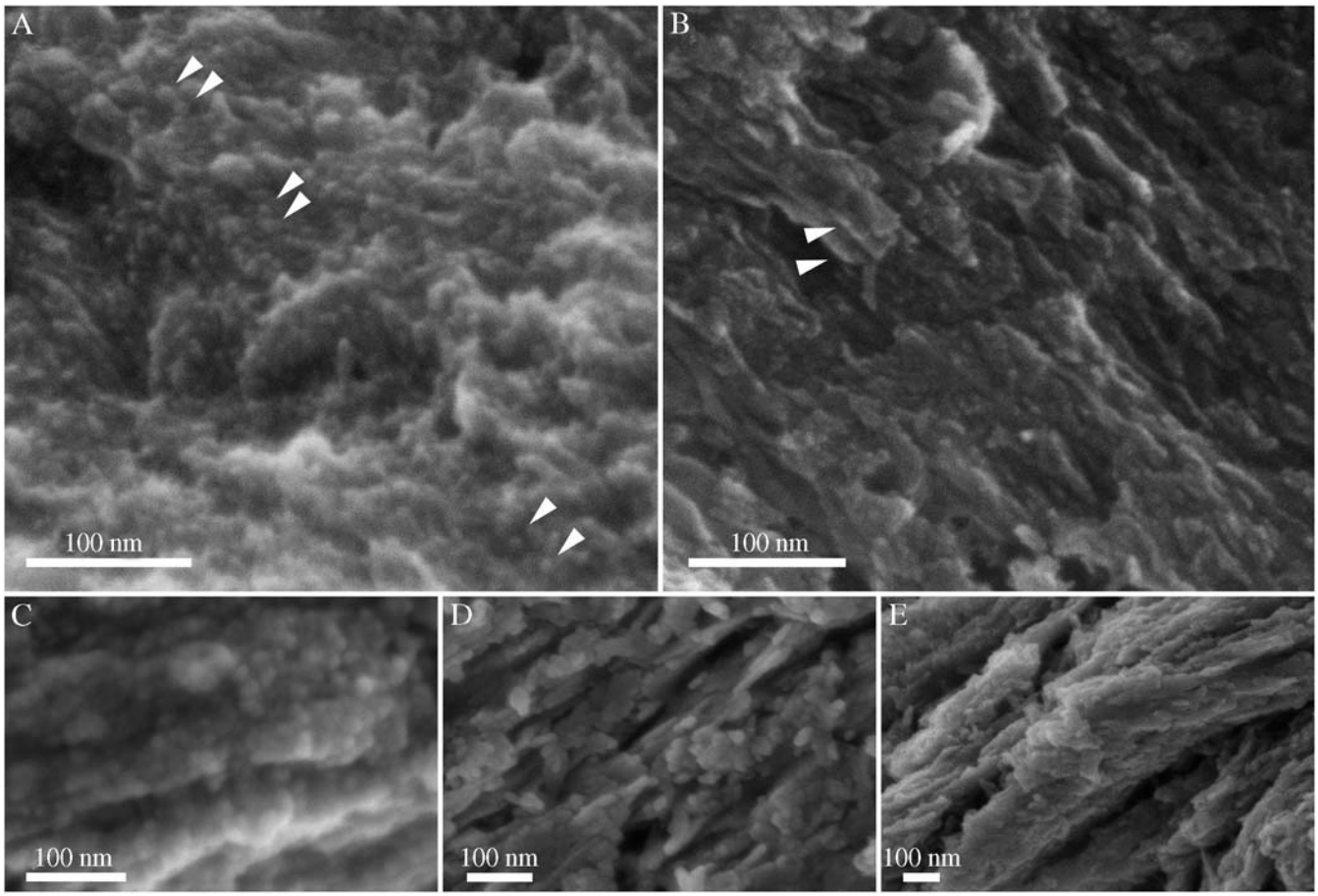

Fig. S5. (*A* and *B*) High resolution cryo-SEM images of newly mineralized and mature-mineralized bone tissue (mineralization is indicated by signal produced in backscattered electrons micrographs; for example, see Fig. S1). (*A*) Distal, newly mineralized bone showing spherical mineral particles (arrowheads, in agreement with the SAXS of amorphous particles in Fig. 3*E*). (*B*) More mature bone showing mineral particles in the shape of thin platelets (arrowheads, in agreement with the SAXS of crystalline particles in Fig. 3*D*). (*C*–*E*) High resolution SEM micrographs showing selected mineral morphologies in young to mature (*C*–*E*, respectively) bone fragments that were bleached to remove the organic matrix and observed dry (as described in ref. 1). (*C*) Newly formed bone mineral is typically formed of spherical particles, with a diameter of 15–20 nm (similar to *A*. Particles in *A* appear smaller, probably because they are partially embedded in the organic matrix and/or in amorphous ice). The dry extracted spherulites were found to be composed of ACP on the basis of electron diffraction and Ca/P ratio. (*D* and *E*) More mature bone mineral particles, from intermediate and mature segments, respectively, exhibit the typical thin platelet morphology of bone apatite crystallites (similar to *B*).

1 Mahamid J, Sharir A, Addadi L, Weiner S (2008) Amorphous calcium phosphate is a major component of the forming fin bones of zebrafish: Indications for an amorphous precursor phase. *Proc Natl Acad Sci USA* 105:12748–12753.